Materials Chemistry and Physics 248 (2020) 122930

Contents lists available at ScienceDirect

Materials Chemistry and Physics

journal homepage: www.elsevier.com/locate/matchemphys

Triblock copolymer grafted Graphene oxide as nanofiller for toughening of epoxy resin

Jitha S Jayan [a], Appukuttan Saritha [a,*], B.D.S. Deeraj [b], Kuruvilla Joseph [b]

[a] Department of Chemistry, School of Arts and Sciences, Amrita Vishwa Vidyapeetham, Amritapuri, Kollam, Kerala, India
[b] Department of Chemistry, Indian Institute of Space Science and Technology Valiamala, Thiruvananthapuram, Kerala, India

HIGHLIGHTS

- Synthesis of triblock copolymer grafted Graphene oxide.
- Incorporation of the grafted filler into the epoxy matrix.
- Analysis of the micellar nanostructures developed using microscopic techniques.
- Correlating the nanostructures developed in epoxy matrix with the improved fracture toughness.

GRAPHICAL ABSTRACT

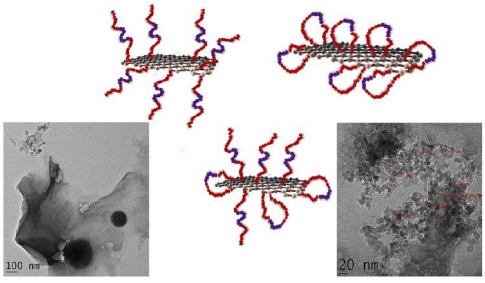

ARTICLE INFO

Keywords:
Graphene oxide
Block copolymer
Toughening
Fracture toughness
Tensile strength

ABSTRACT

Inspired by the mechanical strength produced by Graphene oxide (GO) and Polyethylene Glycol-b-Polypropylene Glycol-b-Polyethylene Glycol (TBCP) block copolymer separately in epoxy composites, we have incorporated both these materials in the form of a graft (GO-g-TBCP) in epoxy. This idea of exploiting the synergistic effect of nanofiller and block copolymer in the form of a graft in the epoxy matrix is a maiden attempt. The grafting process was confirmed through FTIR, FTNMR, XPS, XRD and Raman spectroscopy. Both GO-g-TBCP and GO were incorporated into epoxy and the mechanical properties of the composites were analysed. The fracture toughness showed a tremendous improvement of about 400% without affecting the inherent tensile properties. GO-g-TBCP toughened epoxy displayed about 100% improvement in storage modulus and 33% improvement in tensile strength. These enhanced properties were explained by probing into the sequential arrangement of the nanostructures into a fractal-like structure with the help of HRTEM and SEM micrographs.

1. Introduction

Epoxies are potential thermosets with multidisciplinary applications, but the lower fracture toughness retracts its implementation in many areas [1,2]. For the enhancement of toughness, various materials are employed as a second phase. Elastomers, thermoplastics, organic and inorganic fillers and their hybrids are widely used as reinforcements [3–8]. Fillers having one of the dimensions in the nano regime have replaced these bulk fillers, due to better enhancement in the mechanical properties [9–14]. Nowadays, a class of polymers, known as block copolymers are being employed as toughening agents due to their ability to self-assemble as nanostructures in the epoxy matrix [15–17]. These

* Corresponding author. Department of Chemistry, Amrita School of Arts and sciences, Amrita Vishwa Vidyapeetham.
E-mail address: sarithatvla@gmail.com (A. Saritha).

https://doi.org/10.1016/j.matchemphys.2020.122930
Received 17 January 2020; Received in revised form 12 March 2020; Accepted 14 March 2020
Available online 18 March 2020
0254-0584/

block copolymers can perform a reaction induced microphase separation and can self-assemble into different nanostructures like wormlike micelle, spherical micelle and vesicle depending on the concentration [18–21]. The effective toughening of block copolymers is due to the presence of these nanostructures. Nian et al. [22] recently observed that worm-like micelle is more capable of enhancing the toughness of epoxy than spherical micelle. Block copolymers cause a decrease in tensile properties of the epoxy matrix and this is considered as their major drawback. Poly(ethylene oxide)-poly(propylene oxide)-poly(ethylene oxide) triblock copolymer (PEO-PPO-PEO) is a widely used triblock copolymer (TBCP) due to the reaction-induced microphase separation in the epoxy matrix [23–26]. It consists of two homopolymer units arranged in ABA manner, in which PEO is the crystalline epoxy miscible end and PPO is the amorphous epoxy immiscible end. The amphiphilic nature of this block leads to the formation of different nanostructures in the matrix. Larranga et al. [27] prepared PEO-PPO-PEO block copolymer/epoxy blends and observed an increase in toughness, but the flexural modulus and strength decreased at higher loadings similar to that of rubber modified systems. Tang et al. [28] analysed the effect of reactive poly (glycidyl methacrylate)-b-poly (propylene glycol)-b-poly(glycidyl methacrylate) (GPG) and nonreactive poly(ethylene glycol)-b-poly (propylene glycol)-b-poly(ethylene glycol) on the toughness of epoxy and observed that the reactive blocks are responsible for the well-balanced thermo mechanical properties. Chu et al. [26] confirmed the formation of wormlike micelle of PEO-PPO-PEO block copolymer in epoxy matrix. The high aspect ratio at an optimal length scale of wormlike micelle is responsible for greater toughness than that of other nanostructures. Cano et al. [25] considered the influence of concentration of PEO-PPO-PEO in developing the different nanostructured morphologies in epoxy matrix. The study showed an improvement in the fracture toughness values at 5 wt % of the block with the loss of flexural modulus of epoxy because of the plasticizing effect of the block copolymer. Parameswaranpillai et al. [29] studied the effect of PEO-PPO-PEO on the tensile strength and impact strength of epoxy, and observed an improvement only at higher loadings due to the plasticizing nature of the block. Thus, the block copolymer enhances the toughness of epoxy at higher loadings with compensation of tensile strength. A recent review suggests that the incorporation of nanofiller together with block copolymer might enhance the properties of the epoxy matrix [30]. From the literature it is evident that, simple polymers have been grafted to nanofillers to enhance the properties of epoxy [31–33]. This idea could be applied to block copolymers also.

Graphene is efficient reinforcing filler due to the planar sheet like arrangement of sp^2-bonded carbon atoms in the honeycomb crystal lattice. Graphene Oxide (GO), which is more compatible than graphene due to the presence of functionalities on the surface, is a better option for the grafting process [34,35]. Grafting techniques like 'grafting to' and 'grafting from' can be done to graft the block copolymer onto nanofillers. In the 'grafting from' technique, a macro-initiator is first attached to the nanofiller by means of covalent interaction and the polymerisation of monomers is brought about on the surface [36,37]. In "grafting to" technique, the polymer chains that are synthesised already are attached directly to the functional groups present on the surface of the nanofillers. The surface must be modified chemically to get appropriate functionalities suitable for the grafting process. Gao et al. [38] studied the influence of SiO_2 grafted copolymer of poly (n-hexyl methacrylate)-(poly(glycidyl methacrylate) (PHMA-b- PGMA) in enhancing the mechanical properties like toughness and tensile strength of epoxy. The graft was found to improve the toughness at the expense of the modulus and tensile properties [39]. Li et al. [40] considered the combined effect of graphene as well as PEO-PPO-PEO as fillers in enhancing the toughness without grafting. To the best of our knowledge, this is the first attempt of studying the synergistic effect of GO and TBCP block copolymer in the form of GO-g-TBCP in enhancing the thermo-mechanical properties of epoxy. Though there are several attempts in literature to enhance the toughness of epoxy using block copolymer, none of these works have reported the grafting of nanofiller on to the block copolymer to enhance the properties of the epoxy matrix and hence our earnest approach is to bridge this gap in literature. The incorporation of this grafted system in the epoxy matrix can tailor the properties of the nanocomposite system to make it suitable for high end applications.

2. Experimental

2.1. Materials

Diglycidyl Ether of Bisphenol-A (DGEBA) and curative Diethylene Toluenediamine (DETDA) (CAS No:68479-98-1) were provided by Aditya Birla epoxy division. Graphite powder of 99% purity, PEG-b-PPG-b-PEG triblock copolymer (pluronic @ P-123) of molecular weight (Number average) 5,800 and all other chemicals were obtained from Sigma Aldrich.

2.2. Preparation of GO-g- TBCP

Using commercial graphite as precursor, the filler GO was synthesised by following the well-known Hummer's method [41]. Graphite was oxidized by treating it with H_2SO_4, $NaNO_3$, and $KMnO_4$. H_2O_2 was added to remove the unreacted $KMnO_4$. The product was washed with HCl and water and then dried.

TBCP was grafted onto the surface of GO by ester linkage, after acylating GO using $SOCl_2$. The detailed procedure is shown in Fig. 1. GO was first acylated by refluxing with $SOCl_2$ and the excess of $SOCl_2$ was removed under vacuum. Acylated GO(GO-COCl) was refluxed with the block copolymer TBCP in presence of catalytic amount of Et_3N under N_2 atmosphere using dry THF as solvent. The solvent was removed, washed with THF to remove the unreacted block and then the black solid was separated by centrifugation and dried in vacuum.

2.3. Preparation of epoxy composites

Epoxy composites with calculated amount of GO and GO-g-TBCP loadings were made by dispersing the filler in acetone by means of sonication process followed by the incorporation into DGEBA resin. After mixing, the free solvent was removed with the help of a vacuum pump. Addition of the curative DETDA (DGEBA: DETDA:100:24.4) was subsequently followed by pre and post curing at 140 °C and 200 °C respectively (Fig. 2).

3. Characterization techniques

The grafting of block copolymer onto the surface of GO was confirmed by techniques such as Fourier Transform Infrared Spectroscopy (FTIR), Nuclear Magnetic Resonance (NMR) spectroscopy, X-Ray Diffraction (XRD), X-Ray Photoelectron Spectroscopy (XPS) and Raman spectroscopy. FTIR experiments were carried out in Perkin Elmer Spectrum 2 in ATR mode. Proton NMR was performed using an 800 MHz FT NMR instrument in dimethyl sulphoxide. The Raman spectrum was taken using Alpha 300 RA Raman from 100 to 3000 cm^{-1} using a 532 nm DPSS-Nd:YAG laser following 10 accumulations. Crystal structure of the modified fillers were analysed with the help of X-ray diffractometer (PANalytical 3 kW X'pert PRO). Ultra DLD spectrometer was used to carry out X-ray Photoelectron Spectroscopic (XPS) analysis using Al Kα excitation radiation emitted from Kratos Axis. Scanning Electron Microscopy (SEM) images of the modified filler and fractured surfaces were analysed using TESCAN VEGA3 SB. Jeol/JEM 2100 was used to take High Resolution Transmission Electron Microscopic (HRTEM) images using LaB_6 as source. Phase contrast microscopy was carried out using CX41 Olympus Phase contrast Trinocular microscope. Atomic Force Microscopy (AFM) was carried out using WITec alpha 300RA (WITec GmbH, Ulm, Germany) in non-contact mode.

The tensile strength, modulus and elongation of break of neat epoxy

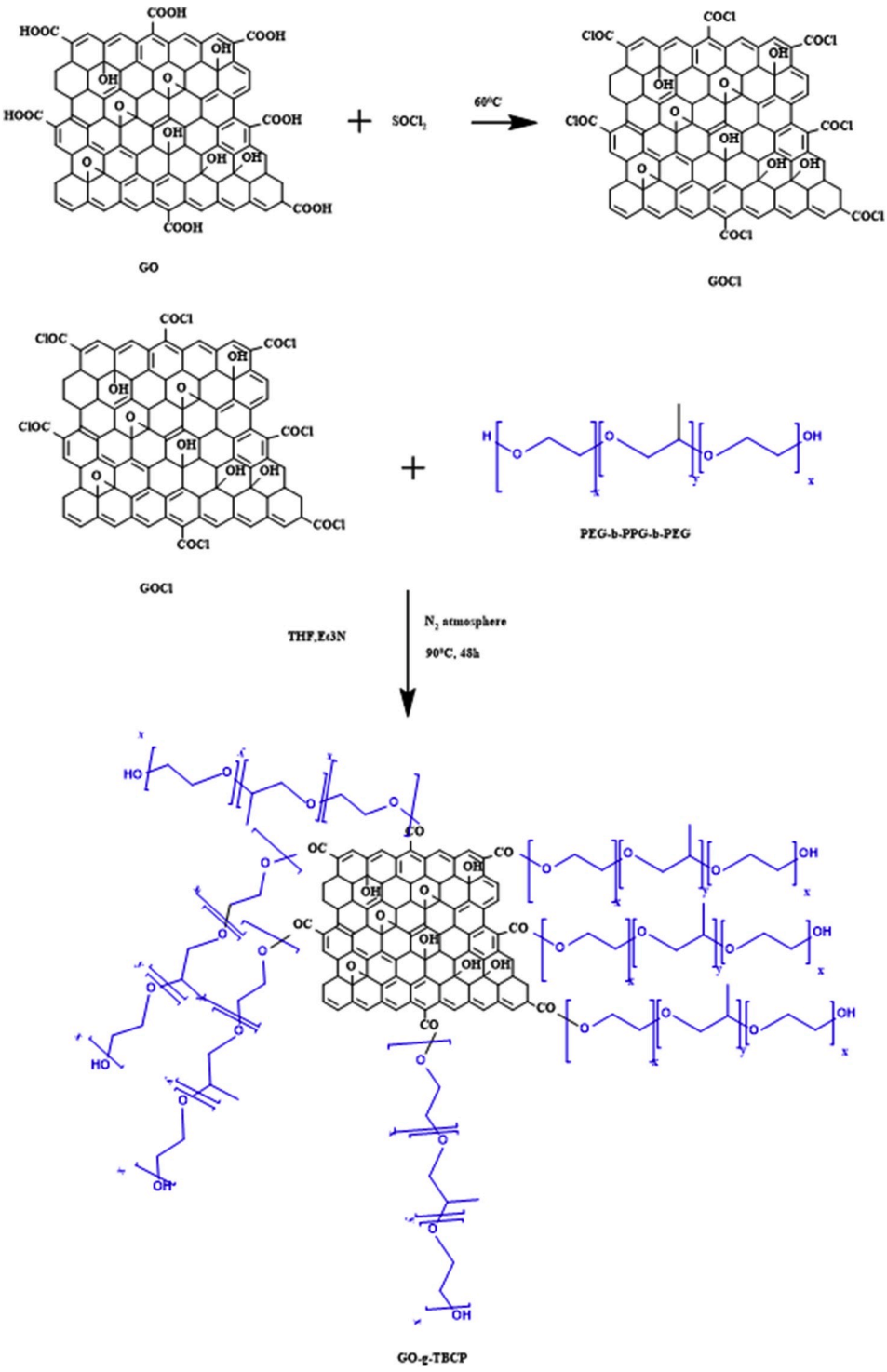

Fig. 1. Schematic representation of the synthesis of GO-g-TBCP.

samples were tested using a UTM by following the ASTM standard D638 (Instron 5984, Instron, USA). The testing speed was maintained at 1 mm/min and gauge length 100 mm. Dog bone shaped samples of 165× 12.7 × 3.2 mm^3 were prepared using Teflon mould for this purpose. UTM (Instron 5984, USA) was used to measure the fracture toughness of the samples at a crosshead speed of 10 mm/min (as per ASTM standard D5045). Single edge notch specimens of 50 mm × 10 mm x 5 mm were used to measure the fracture toughness. The test results of five samples were taken and average was noted in all the cases. The fracture toughness is expressed in terms of stress intensity factor (K_{IC}), which is calculated using equation (1) [42,43].

$$K_{IC} = \frac{L}{BW^{0.5}} f(x) \tag{1}$$

Where,

$$f(x) = \frac{6x^{0.5}[1.99 - x(1-x)(2.15 - 3.93x - 2.7x^2]}{(1+2x)(1-x)^{1.5}} \tag{2}$$

and *L, B, W* and a are the load at crack initiation, specimen thickness, specimen width and crack length respectively. x is the crack length to

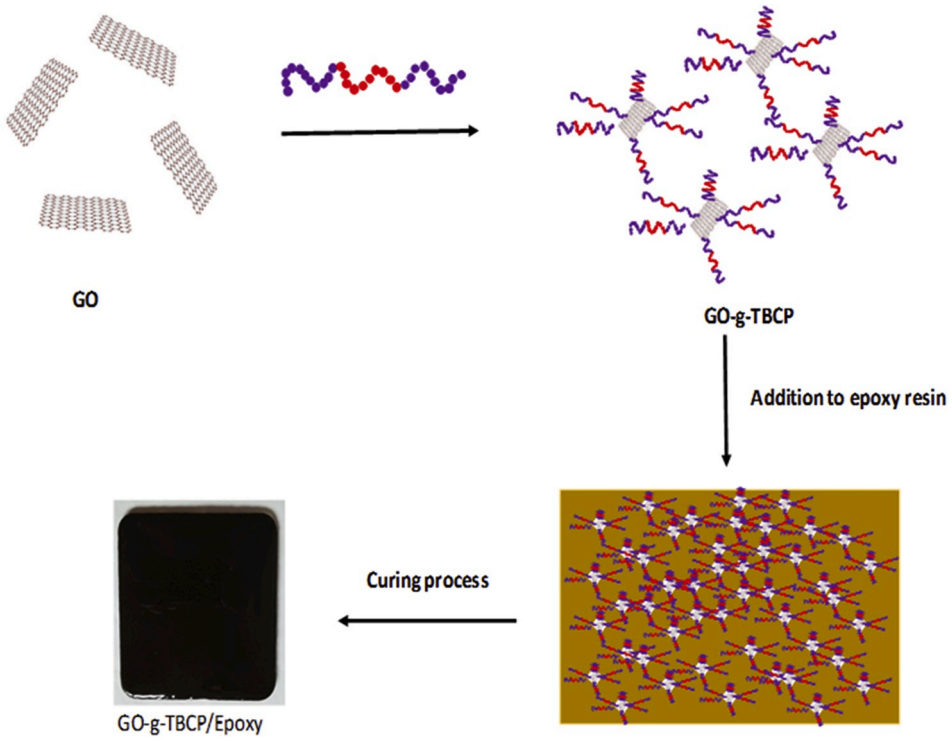

Fig. 2. Schematic representation of Synthesis of GO-g-TBCP/Epoxy composites.

width ratio.

Dynamic Mechanical Analyzer (Perkin Elmer) was used to analyse the loss modulus, storage modulus and mechanical damping factor of the fabricated epoxy samples and experiments were carried out in tension mode. The examination was performed from 30 °C to 250 °C at a heating rate of 2 °C/min at a frequency of 1 Hz.

4. Results and discussions

4.1. FTIR

The grafting of TBCP onto the surface of GO was confirmed by various spectroscopic techniques. Fig. 3a shows the characteristic FTIR spectra of GO [44]. The peaks obtained at 1728 cm^{-1} and 1050 cm^{-1} confirm the presence of C═O and C–O groups respectively. The broad band at 3400 cm^{-1} corresponding to OH groups confirm the oxidation of graphite. Skeletal vibrations are due to the un-oxidized graphitic parts. The peak obtained at about 3400 cm^{-1} for the TBCP confirms the presence of O–H group. The shift in the characteristic band at 1728 cm^{-1} to 1628 cm^{-1} in the GO-g-TBCP also confirms the grafting of GO onto the block copolymer [45]. The pronounced peak at about 3400 cm^{-1} seen in the GO-g-TBCP confirms the grafting process. The C–O–C stretching vibration obtained for GO-g-TBCP confirms the grafting process and the formation of the nanohybrid.

4.2. NMR

^{1}HNMR results obtained for the nanohybrid helped to ratify the grafting process. The peak obtained at $\delta \sim 3.5$ ppm is due to the proton signal of (-O- $(CH_2)_2$–O-) and (-O–CH_2–) in the TBCP and the sharp peak obtained at $\delta \sim 2.5$ is due to the solvent. The small peak obtained at $\delta =$ 2.5 ppm is due to the –CH_3 in the propylene group of the block copolymer. The peak obtained at $\delta \sim 4.38$ ppm is because of the presence of protons in GO. Hence it is evident that the grafting of block copolymer

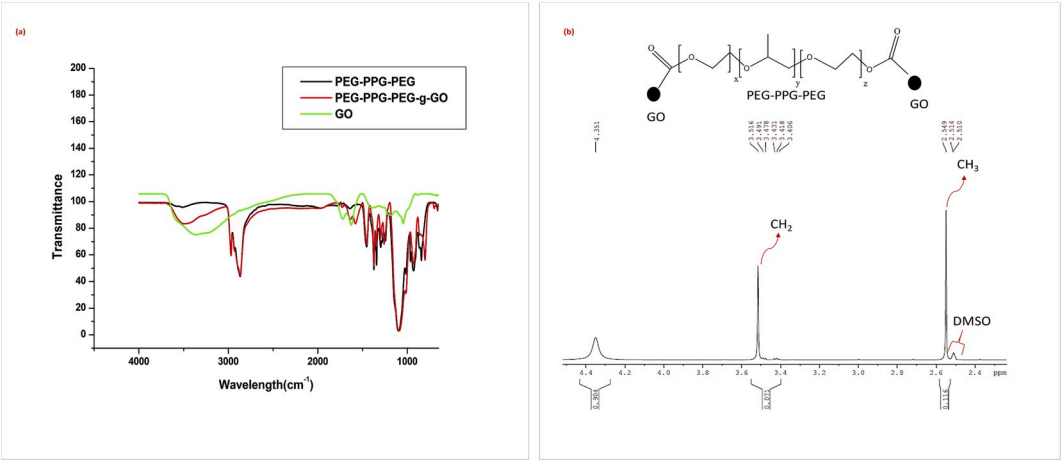

Fig. 3. (a) FTIR and (b)NMR spectra of GO-g-TBCP.

onto the GO surface (through the 'grafting to' technique) is through the –OH group (Fig. 3b).

4.3. Raman analysis

Raman spectra were taken in order to further substantiate the grafting. There is an increase in the intensity of D band and reduction in the intensity of the G band (Fig. 4a) which clearly confirms the grafting of block copolymer onto GO. There are two pronounced peaks at 1356 cm^{-1} and 1596 cm^{-1} corresponding to D and G band due to the sp^2 carbon and κ-point phonons of A1g symmetry respectively. After the grafting of GO with the block copolymer, the intensity of D band is increased and that of G band is reduced confirming the attachment of the triblock copolymer. This can be further confirmed from the increase in I_D/I_G ratio. The I_D/I_G ratio of GO is showing an enhancement from 1 to 1.2 after the grafting process [46]. Another pronounced peak obtained for graphite at 2700 cm^{-1} corresponds to the 2D band. After grafting the nano filler with the block copolymer, the 2D band splits into two, showing peaks at 2650 cm^{-1} and 2910 cm^{-1} respectively. The splitting is associated with the splitting of electron dispersion energies and it is due to the interaction of neighbouring graphitic planes [47,48]. Hence the formation of nanohybrids of GO-g-TBCP is substantiated from the Raman spectra.

4.4. XRD studies

XRD pattern of graphite depicts a peak at 26.315° which corresponds to an interlayer spacing of 0.3384 nm (Fig. 4b) due to the (002) plane. After oxidation, the peak is shifted to 9.03° as a result of the increase in the interlayer spacing (1.27 nm) due to the functionalization of the graphite surface. The peak at 9.03° confirms the formation of GO. The absence of reflection peak at 26.315° in GO confirms the presence of disordered graphitic sheets (Fig. 4c) [49]. The peak at 20° in GO-g-TBCP nanohybrid confirms the absence of crystallinity in graphite due to the intercalation of TBCP block copolymer into the graphitic layers. As a result of intercalation of the block copolymer, the interlayer spacing shifts from 0.208 nm to 0.5961 nm. In the case of GO-g-TBCP, the peak at 26.315° is completely absent. This clearly indicates the intercalation of TBCP in between the graphitic layer and its subsequent exfoliation as few layer thick graphene sheets. As a result of exfoliation, the ordered structure is lost, and the system now exists as few layer thick intercalated graphene sheets. By comparing TGA results (Fig. S1) of GO and GO-g-TBCP, the graft density of GO-g-TBCP is 1.146 g (i.e. 0.17graft/g).

4.5. XPS studies

XPS gives a clear picture of the grafting process. Fig. 5a compares the C^1s spectra of GO and GO-g-TBCP nanohybrid. From the C^1s spectra, the peak obtained at 288.82 eV (O–C═O), 286.79 eV (C═O) and the peak due to the sp^2 carbon atom (284.46eV) confirms the formation of GO from graphite (Fig. 5b) [49]. From the XPS data obtained, it is clear that the peak obtained at 288.82 eV is shifted to 288.64 in the case of TBCP grafted GO and the intensity of the peak is reduced confirming the chlorination followed by grafting of TBCP onto it (Fig. 5c). The acylation of carboxyl groups of GO is evident from the intensity of the peak at 288.82 eV. Due to acylation, the –OH of the carboxylic group is converted to –Cl and the overall intensity of O–C═O is reduced. This confirms the acylation using $SOCl_2$. The peak of C═O is shifted to a lower region, due to grafting of TBCP which increases the electron density and in turn leads to a reduction in binding energy. The increased intensity confirms the grafting process. Further, the ratio of the intensity of the peak of GO to that of GO-g-TBCP at 284eV is 1.4, confirming the grafting of TBCP. Fig. 5d shows the increased oxygen intensity after the grafting process.

The morphology of the graft was analysed using techniques like TEM, SEM, AFM and Phase Contrast Microscopy. This helps in giving a

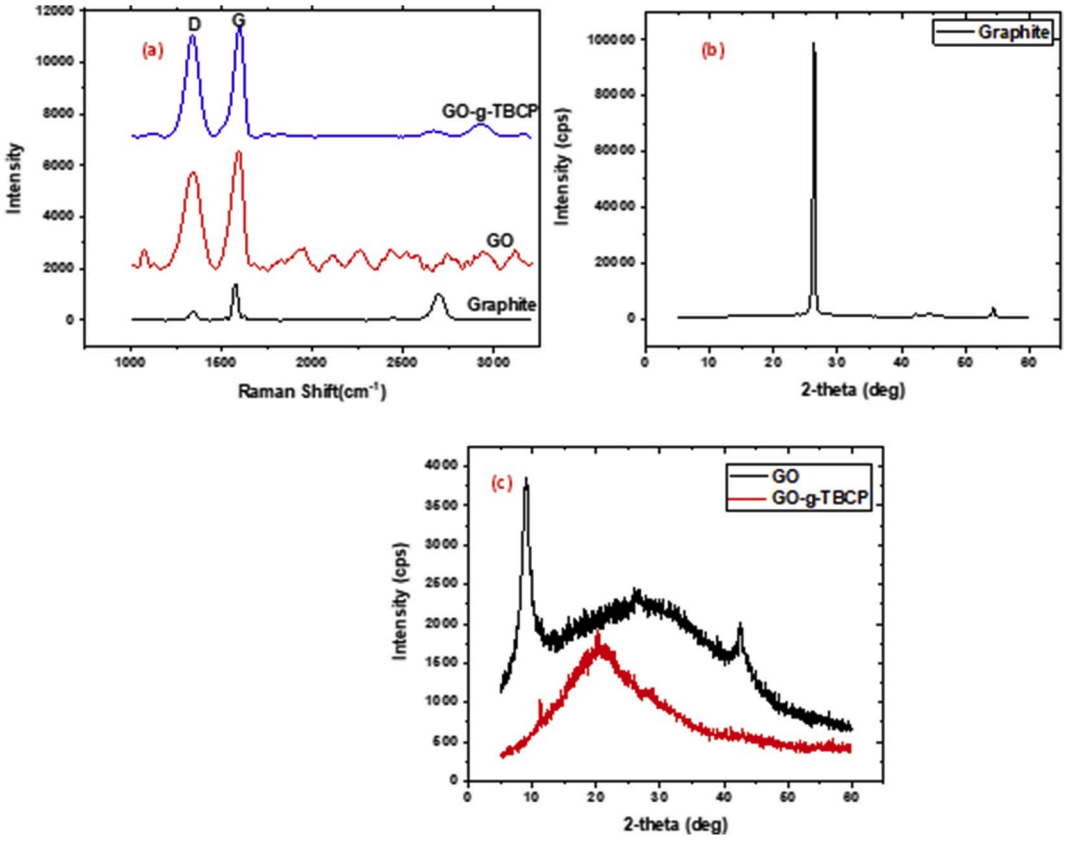

Fig. 4. Raman and XRD spectra of GO and GO-g-TBCP.

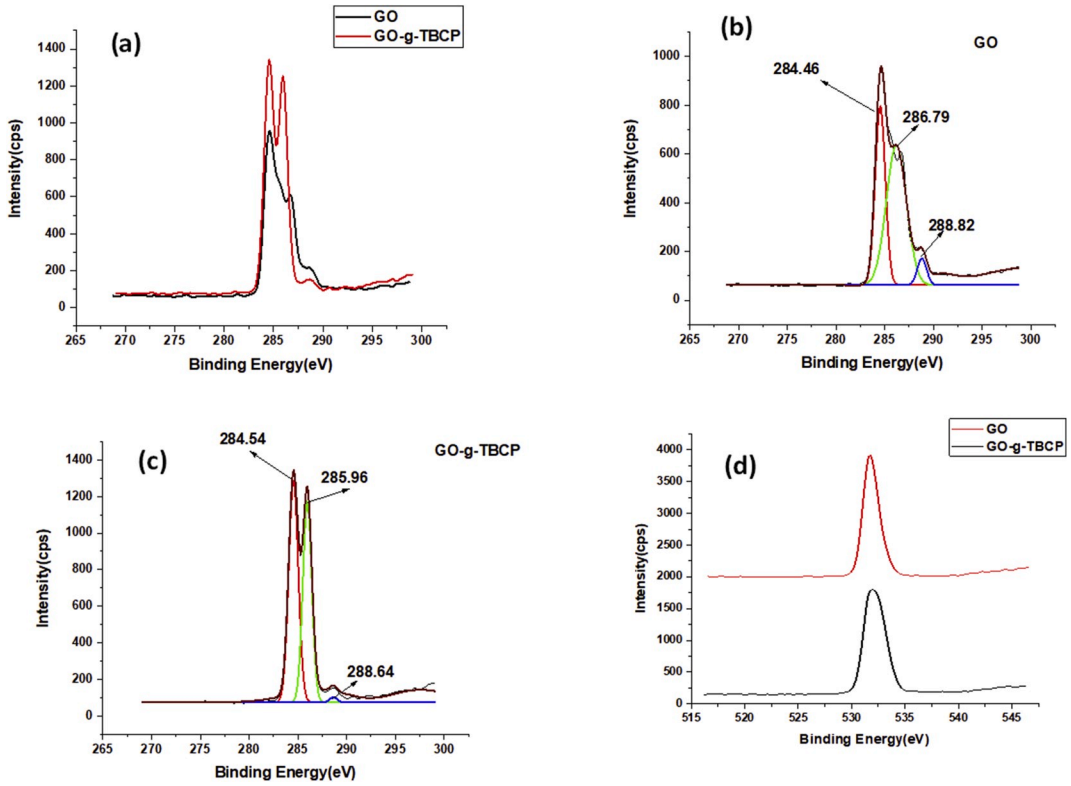

Fig. 5. (a) XPS spectra of GO and GO-g-TBCP, (b) C1s spectra of GO (c) c1s spectra of GO-g-TBCP, (d) O spectra of GO and GO-g-TBCP.

clear picture of the grafted surface and helps to identify the arrangement of the micellar nanostructures. It is seen from literature that block co-polymers assemble to form worm-like or spherical micelle in the epoxy matrix [18,50]. The interesting part of this work is that the grafting process itself has initiated the formation of micelle in the filler. The HRTEM images of the GO-g-TBCP shown in Fig. 6a, confirms the grafting process as well as the arrangement of the micellar structures. It is very interesting to note that the grafting process is the driving force towards the formation of micelles. This can be clearly understood from the TEM images which depict the formation of nanostructured spherical micelles having a diameter range of 6–11 nm. Each of the spherical micelle contains the grafted GO inside it and this can be observed from the AFM images in Fig. 6b. The SEM and phase contrast images (Fig. S2) of the nanohybrid confirms the observation obtained from HRTEM and AFM analysis. The grafted filler assembles in the form of a spherical micelle where GO gets entrapped inside. The grafting of block copolymer onto the GO layers enhances the dispersion of GO in acetone, water etc. and hence the dispersion in epoxy can be achieved easily.

4.6. DMA (dynamic mechanical analysis)

The DMA results show an enhancement in the glass transition temperature (Tg). The tan δ curve as shown in Fig. 7a shows an increase in Tg. As the loading increases, there is an increase in Tg, due to the higher crosslinking density of the polymer chains. The presence of two peaks in tan δ curve obtained for the grafted filler loaded epoxy is due to the existence of different polymer networks. The presence of TBCP in the epoxy network in the form of a graft is responsible for the additional peak in the tan δ curve. The second peak is attributed to the plasticizing effect of TBCP (Fig. 7c). In the case of obtaining two different peaks, the

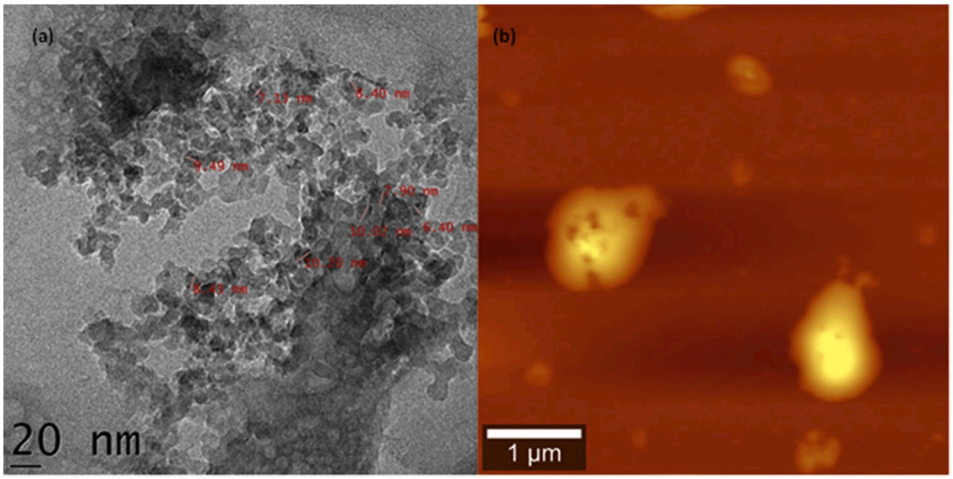

Fig. 6. HRTEM and AFM images of GO-g-TBCP.

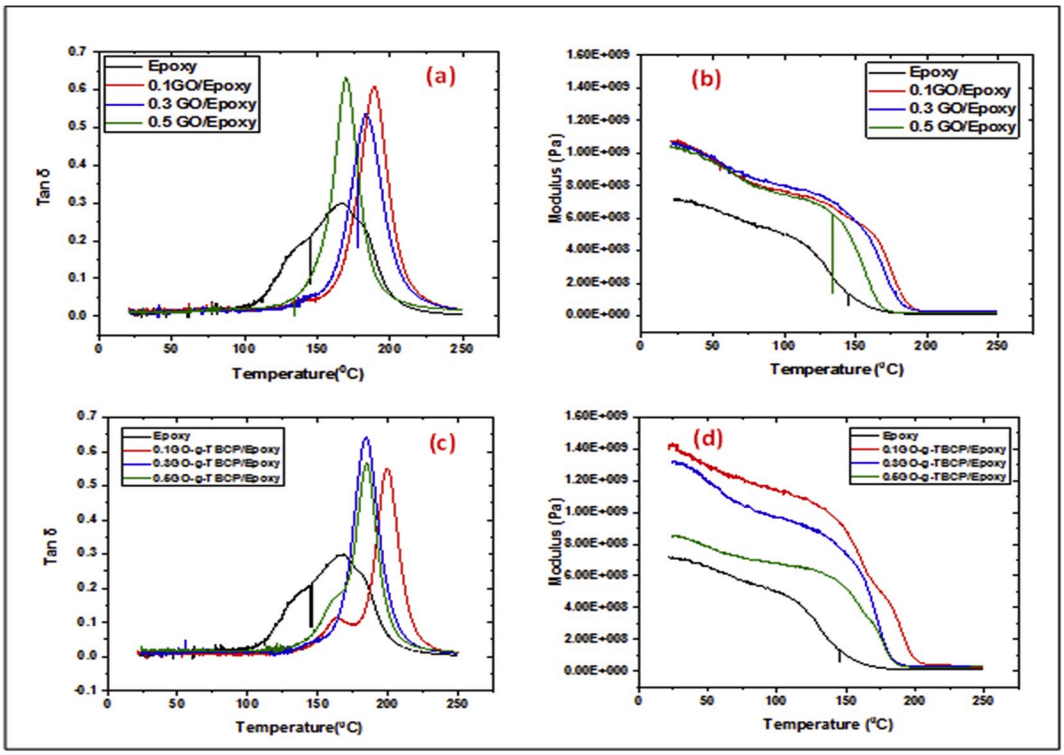

Figure 7. (a) and (b) Tan δ and Storage modulus of GO/Epoxy composites, (c) and (d) Tan δ and storage modulus of GO-g-TBCP/epoxy composites obtained from DMA analysis.

higher Tg value, will have to be taken into consideration. The obtained results were compared with that of toughened epoxy GO composites and it was observed that the Tg values first increases and then decreases in both the cases. The increase in Tg is due to the confinement of epoxy chains onto the surface of nanosheets and thus it reduces the chain mobility and works like a physical interlock. Moreover, the functionalities over the filler can also take part in the curing process and thus enhance the Tg value [51]. Higher loadings of filler lead to aggregation and badly effects the confinement leading to a reduction in Tg [52]. The same trend is observed for GO-g-TBCP toughened epoxy composites. Generally, block copolymers do not have a pronounced effect on Tg. The PEO and the mobile PPO part of the TBCP generally reduces the Tg due to less crosslinking [53,54]. Hence as the loading of the graft increases, the Tg shows a reduction. But the reduction is not in so prominent due to the combined effect of GO and TBCP.

The storage modulus of the epoxy (Fig. 7b,d) is tremendously improved by the addition of both the fillers. 0.1 wt% graft loaded epoxy composites show an overall improvement of about 100% in storage modulus, whereas it is only 51.42% in the case of GO alone toughened system.

Crosslink density ν is calculated by equation (3) [55,56],

$$\nu = \frac{E_r}{3RT_r} \tag{3}$$

Where T_r is the temperature above T_g, E_r is the storage modulus corresponding to T_r obtained from DMA data and R is the real gas constant. The calculated crosslink density has a unit of mol/m^3. The obtained results are tabulated in Table 1. Molecular weight between crosslinks (M_c) was also determined from the DMA data. Molecular weight between crosslinks was calculated using equation (4) [57].

$$M_C = \frac{3RT_r d}{E_r} \tag{4}$$

Where d is the polymer density. The results show that the incorporation of GO as well as GO-g-TBCP reduces the crosslink density. Decreased crosslink density is associated with increase in Tg value. The reason behind the increased Tg with decreased crosslink density is due to the restricted mobility at the interface due to the attractive interactions between the epoxy and the nanoparticle. This is due to the disruption of the crosslinking network by the nanoparticle [58]. Similar observation is obtained for GO-g-TBCP incorporated epoxy as well. In all the cases, the lower crosslink density is associated with higher Mc values. Toughenability of the epoxy composite is increased with decrease in crosslink density and is in accordance with the literature results [59].

Table 1
Glass transition temperature obtained from DMA.

Filler	Loading (wt %)	Tg (°C)	Crosslink density(ν)	Molecular weight b/w crosslinks (M_c)
GO	0	168	3820.962	0.0001
	0.1	190	1982.293	0.0002
	0.3	170	2444.297	0.0002
	0.5	184	1528.529	0.0003
GO-g-TBCP	0	168	3820.962	0.0001
	0.1	200	2032.927	0.00004
	0.3	185	2505.862	0.0005
	0.5	185	2052.715	0.0009

4.7. Fracture toughness

The results obtained while analysing the fracture toughness were exciting and the improvement in toughness was superior to that obtained for GO and block copolymer alone in the epoxy matrix. The GO-g-TBCP, functioned efficiently and synergistically as a reinforcement than GO and the block copolymer in individual form. The incorporation of GO as well as the GO-g-TBCP enhances the toughness of epoxy to a greater extent, but it is noteworthy that the grafting of block onto GO makes it a more efficient filler without diminishing the inherent elastic properties. GO enhances the toughness to about 255.24% at 0.1 wt%, whereas at

higher loadings toughness decreases due to the agglomeration of GO as shown in Fig. 8. As the loading of GO-g-TBCP increases, the fracture toughness keeps on increasing and a maximum of 400% improvement is obtained. When compared to neat epoxy, the development of micelle in the GO-g-TBCP filled epoxy system is responsible for the toughness enhancement. After an extensive bibliographic review, none of the studies with block copolymer has shown such an enhancement in toughness as reported in the present work. When Larranga et al. [23] used the same block copolymer for toughening the epoxy matrix, the toughness of the system increased with the addition of 20% of the block copolymer with a decrease in the tensile strength and flexural properties. Li et al. [40] observed only a 1.7 fold improvement in toughness of epoxy composites by using graphene and Poly (ethylene-alt-propylene)-b-(poly ethylene oxide) in the un-grafted form.

The improvement in toughness of the present work can be explained by the gigantic micellization of GO-g-TBCP with in the epoxy matrix during the curing process as observed from TEM images. For lower loadings of the graft, the micelles formed were of spherical shape and they form caterpillar like aggregates. As the concentration increases, the filler self-assemble into wormlike form and transforms later into octopus like gigantic aggregates having wormlike micellar tentacles. The epoxy gets trapped inside the aggregates which act as barriers for crack propagation. The improvement in toughness is tabulated in Table 2. The enhancement of toughness obtained in the present work is compared with the already reported works and is presented in Table 3.

4.8. Tensile strength

The tensile strength of GO grafted epoxy composites shows a steady improvement with filler loading. Usually, the triblock copolymer, due to its plasticization effect reduces the tensile strength of epoxy composites [60]. But as we grafted the soft TBCP with more stiff GO, the fracture toughness as well as the tensile properties showed an improvement. As the loading of the grafted filler increases, the effect of GO starts to act together with micellization and aggregation leading to the formation of octopus like gigantic aggregates [61,62]. At higher loadings, the nano-filler content present in the graft increases and it nullifies the negative effect on tensile properties.

Thus for 0.5 wt% of GO-g-TBCP, the improvement in tensile strength is about 32.7%. For the same loading of GO, the improvement is only 24.96%. Thus it is evident that grafting enables GO to exhibit superior mechanical properties in the epoxy matrix (Table 2) due to the development of nano structures [63].

Table 2
Mechanical properties such as fracture toughness and tensile strength of GO and GO-g-TBCP toughened epoxy.

Filler loading (wt%)	Fracture Toughness (K_{IC}) ($MPam^{1/2}$)		Tensile Strength (MPa)	
	GO	GO-g-TBCP	GO	GO-g-TBCP
0	1.43 ± 0.2	1.43 ± 0.1	42.3 ± 0.1	42.3 ± 0.0
0.05	3.90 ± 0.2	3.93 ± 0.2	49.3 ± 0.1	41.3 ± 0.2
0.1	5.08 ± 0.11	3.99 ± 0.2	51.4 ± 0.1	39.8 ± 0.1
0.3	4.53 ± 0.1	4.60 ± 0.3	46.3 ± 0.1	45.03 ± 0.1
0.5	2.72 ± 0.1	7.12 ± 0.1	52.86 ± 0.1	56.13 ± 0.1

Table 3
Fracture toughness in comparison with existing polymer/GO toughened epoxy systems.

Polymer grafted GO system in epoxy	Block copolymer/ GO in epoxy	Toughness obtained	Reference
GO-g-PAA		87%	Sahu et al. [64]
GO-g-CTBN		128%	Konnola et al. [65]
GO-g-DGEBA		26%	Wan et al. [66]
GO-g-HPEEK		31%	Katti et al. [67]
GO-g-PEG		334%	Jayan et al. [68]
	GO/PEO-PPO	170%	Li et al. [40]
	rGO/PCL-PPC-PCL	60%	Liu et al. [69]
	GO-g-PEG-PPG-PEG	**400%**	**Current result**

4.9. Morphology of GO-g-TBCP in epoxy

The morphology of the epoxy composites as well as the enhancement in toughness can be monitored and explained in detail with the help of high resolution TEM images. It can be seen from Fig. 9a that for the neat epoxy there is no micelle formation. As the graft is incorporated into the matrix, they start to aggregate into micelle. In the case of lower loadings, the grafted filler self-assembles to form spherical micelle due to the amphiphilic nature of TBCP. Epoxy-phobic PPG and epoxy-philic PEG will self-assemble due to reaction induced phase separation and form spherical micelle which contains the grafted GO with PEG as core and the epoxy-phobic PPO as corona. But as loading increases, the micelle aggregates to form caterpillar, worm and finally transform into octopus

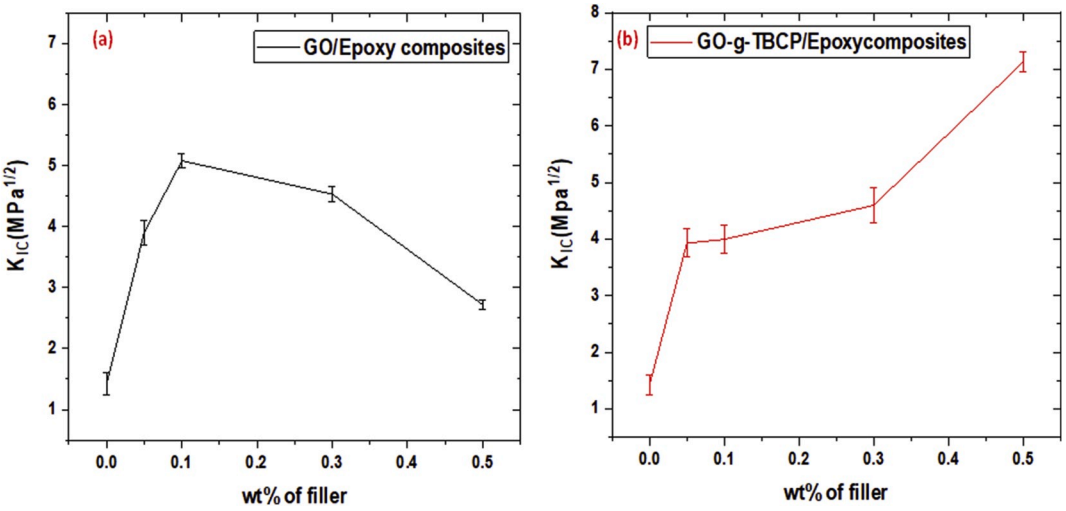

Fig. 8. Fracture toughness of GO/Epoxy and GO-g-TBCP/Epoxy.

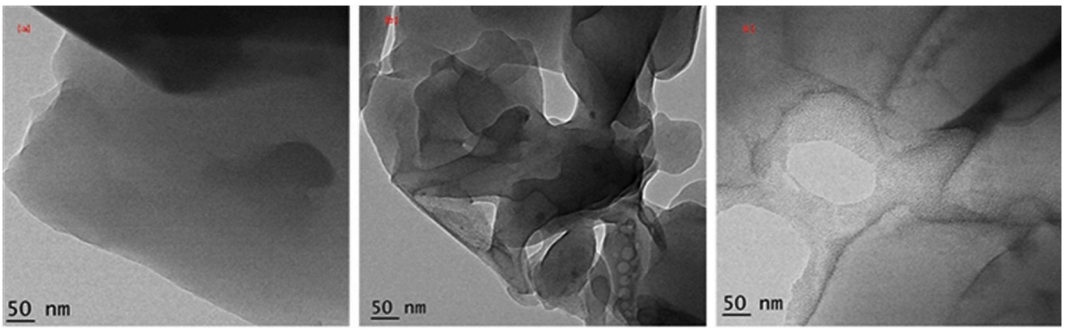

Fig. 9. HRTEM images of ultra-microtomic cross sections of (a) neat epoxy, (b) 0.1 wt% of GO-g-TBCP toughened (c) 0.5 wt% of GO-g-TBCP toughened epoxy.

like arrangements (fractal structures) as shown in Fig. 9. As octopus formation (higher loadings) is due to the aggregation of GO-g-TBCP, the enhancement in toughness will be much higher than that observed for the spherical ones (lower loadings). As reported by researchers, the fractal structures are very effective in enhancing the crack strength as well as residual loading capacity of composites [70]. These hierarchical arrangements lead to complex geometry due to the interlocked topography [71–73]. Hence the aggregates that are forming fractal structures in the epoxy resin contribute towards the enhancement in fracture toughness and tensile strength.

SEM images of the fractured surface give idea about the toughening mechanism. The plane fracture surface of the neat system (Fig. 10 a,d,g) confirms the brittle fracture and thereby shows the poor toughening in neat epoxy. In the case of GO loaded system, the crack deflection and crack pinning are visible from the SEM micrographs (Fig. 10 b,e,h). Coarseness, ditches and parabolic features in the micrographs help in the identification of the toughening mechanism. The grafted filler shows much higher toughness than the other systems due to the combined effect of crack deflection, cavitation, crack pinning and particle pull out. From Fig. 10 c and 10f and 10 i, the mechanism of toughness can be identified evidently as debonding followed by particle pull out. Cavitation and debonding mechanisms arise due to the presence of micelle in the epoxy matrix. The secondary mechanisms like crack deflection and interlocking further enhances the toughness [16,74]. Compared to spherical micelle at lower loadings, wormlike micelle formed at higher loadings possess a higher diameter and hence shows better enhancement in toughness [75].

5. Conclusion

PEG-b-PPG-b-PEG triblock copolymer was successfully grafted onto the surface of GO, by the 'grafting to' technique. The arrangement of graft in the form of micelle is confirmed through surface analysis techniques like SEM, TEM and AFM. The graft produced an enhancement of about 400% in toughness, 100% in storage modulus and 33% in tensile strength. This improvement produced in the mechanical properties can be attributed to the formation of octopus like aggregates with tentacles as confirmed by HRTEM. The toughening mechanisms are explained

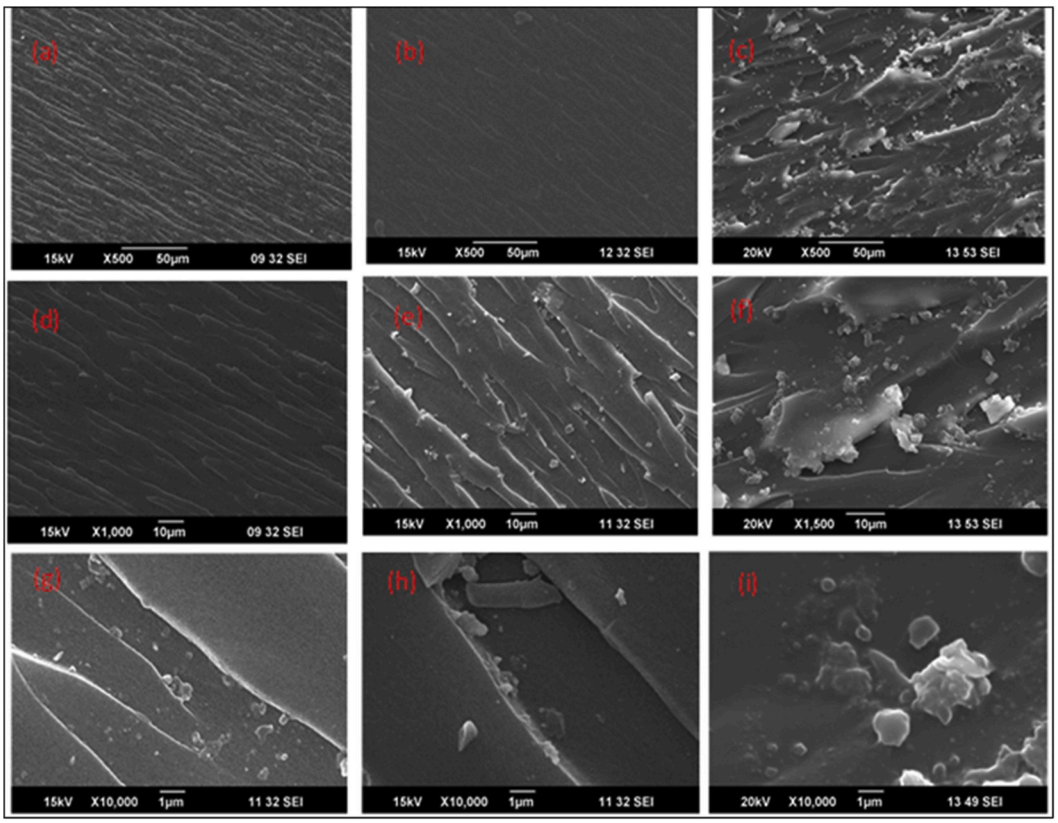

Fig. 10. SEM images of the fractured surface of neat, GO/Epoxy, GO-g-TBCP/epoxy at 50 µm (a, b, c), 10 µm (d, e, f) and 1 µm (g, h, i).

using the SEM micrographs. The DMA of the system also confirms the enhancement in the mechanical properties of the system. The enhancement of toughness in the epoxy matrix via the incorporation of specifically fabricated micellar structures in the form of nano filler grafted block copolymer would definitely enhance the utility of epoxy in high end applications.

Data availability statement

The data that support the findings of this study are available on request from the corresponding author. The data is not publicly available.

Declaration of competing interest

The authors declare that they have no known competing financial interests or personal relationships that could have appeared to influence the work reported in this paper.

CRediT authorship contribution statement

Jitha S Jayan: Conceptualization, Writing - original draft. **Appukuttan Saritha:** Supervision, Writing - review & editing. **B.D.S. Deeraj:** Formal analysis. **Kuruvilla Joseph:** Writing - review & editing.

Acknowledgement

The authors would like to thank Aditya Birla group for supplying the DGEBA and the DETDA hardener for the study. The authors would also like to thank Amrita Vishwa Vidyapeetham for the financial support.

Appendix A. Supplementary data

Supplementary data to this article can be found online at https://doi.org/10.1016/j.matchemphys.2020.122930.

References

[1] F. Hussain, M. Hojjati, M. Okamoto, R.E. Gorga, Polymer-matrix nanocomposites, processing, manufacturing, and application: an overview, J. Compos. Mater. 40 (17) (2006) 1511–1575.
[2] Y. Rao, S. Ogitani, P. Kohl, C.P. Wong, Novel polymer–ceramic nanocomposite based on high dielectric constant epoxy formula for embedded capacitor application, J. Appl. Polym. Sci. 83 (5) (2002) 1084–1090.
[3] M. Franco, I. Mondragon, C.B. Bucknall, Blends of epoxy resin with amine-terminated polyoxypropylene elastomer: morphology and properties, J. Appl. Polym. Sci. 72 (3) (1999) 427–434.
[4] J.H. Hodgkin, G.P. Simon, R.J. Varley, Thermoplastic toughening of epoxy resins: a critical review, Polym. Adv. Technol. 9 (1) (1998) 3–10.
[5] S. Fellahi, N. Chikhi, M. Bakar, Modification of epoxy resin with kaolin as a toughening agent, J. Appl. Polym. Sci. 82 (4) (2001) 861–878.
[6] A. Mirmohseni, S. Zavareh, Preparation and characterization of an epoxy nanocomposite toughened by a combination of thermoplastic, layered and particulate nano-fillers, Mater. Des. 31 (6) (2010) 2699–2706.
[7] F.-L. Jin, S.-J. Park, Thermal properties of epoxy resin/filler hybrid composites, Polym. Degrad. Stabil. 97 (11) (2012) 2148–2153.
[8] T. Kawaguchi, R.A. Pearson, The effect of particle–matrix adhesion on the mechanical behavior of glass filled epoxies. Part 2. A study on fracture toughness, Polymer 44 (15) (2003) 4239–4247.
[9] Y.T. Park, Y. Qian, C. Chan, T. Suh, M.G. Nejhad, C.W. Macosko, A. Stein, Epoxy toughening with low graphene loading, Adv. Funct. Mater. 25 (4) (2015) 575–585.
[10] B.T. Marouf, Y.-W. Mai, R. Bagheri, R.A. Pearson, Toughening of epoxy nanocomposites: nano and hybrid effects, Polym. Rev. 56 (1) (2016) 70–112.
[11] Q.M. Jia, M. Zheng, C.Z. Xu, H.X. Chen, The mechanical properties and tribological behavior of epoxy resin composites modified by different shape nanofillers, Polym. Adv. Technol. 17 (3) (2006) 168–173.
[12] S.G. Prolongo, M.R. Gude, A. Urena, Water uptake of epoxy composites reinforced with carbon nanofillers, Compos. Part A Appl. Sci. Manuf. 43 (12) (2012) 2169–2175.
[13] C.B. Ng, B.J. Ash, L.S. Schadler, R.W. Siegel, A study of the mechanical and permeability properties of nano-and micron-TiO2 filled epoxy composites, Adv. Compos. Lett. 10 (3) (2001), 096369350101000301.
[14] J.S. Jayan, A. Saritha, R. Sreepriya, K. Joseph, Transport phenomena of graphene oxide modified epoxy nanocomposites using diaminodiphenyl methane as curing agent, in: 2017 Int. Conf. Technol. Adv. Power Energy (TAP Energy), 2017, pp. 1–5.
[15] Z.J. Thompson, M.A. Hillmyer, J. Liu, H.-J. Sue, M. Dettloff, F.S. Bates, Block copolymer toughened epoxy: role of cross-link density, Macromolecules 42 (7) (2009) 2333–2335.
[16] J.M. Dean, P.M. Lipic, R.B. Grubbs, R.F. Cook, F.S. Bates, Micellar structure and mechanical properties of block copolymer-modified epoxies, J. Polym. Sci., Part B: Polym. Phys. 39 (23) (2001) 2996–3010.
[17] J.D. Liu, H.-J. Sue, Z.J. Thompson, F.S. Bates, M. Dettloff, G. Jacob, N. Verghese, H. Pham, Strain rate effect on toughening of nano-sized PEP–PEO block copolymer modified epoxy, Acta Mater. 57 (9) (2009) 2691–2701.
[18] Y.S. Thio, J. Wu, F.S. Bates, The role of inclusion size in toughening of epoxy resins by spherical micelles, J. Polym. Sci., Part B: Polym. Phys. 47 (11) (2009) 1125–1129.
[19] A. Blanazs, S.P. Armes, A.J. Ryan, Self-assembled block copolymer aggregates: from micelles to vesicles and their biological applications, Macromol. Rapid Commun. 30 (4-5) (2009) 267–277.
[20] M.T. Bashar, U. Sundararaj, P. Mertiny, Morphology and mechanical properties of nanostructured acrylic tri-block-copolymer modified epoxy, Polym. Eng. Sci. 54 (5) (2014) 1047–1055.
[21] N. Hameed, Q. Guo, T. Hanley, Y. Mai, Hydrogen bonding interactions, crystallization, and surface hydrophobicity in nanostructured epoxy/block copolymer blends, J. Polym. Sci., Part B: Polym. Phys. 48 (7) (2010) 790–800.
[22] F. Nian, J. Ou, Q. Yong, Y. Zhao, H. Pang, B. Liao, Reactive block copolymers for the toughening of epoxies: effect of nanostructured morphology and reactivity, J. Macromol. Sci. Part A 55 (7) (2018) 533–543.
[23] M. Larrañaga, E. Serrano, M.D. Martin, A. Tercjak, G. Kortaberria, K. de la Caba, C. C. Riccardi, I. Mondragon, Mechanical properties–morphology relationships in nano-/microstructured epoxy matrices modified with PEO–PPO–PEO block copolymers, Polym. Int. 56 (11) (2007) 1392–1403.
[24] J. Parameswaranpillai, S.P. Ramanan, S. Jose, S. Siengchin, A. Magueresse, A. Janke, J. Pionteck, Shape memory properties of epoxy/PPO–PEO–PPO triblock copolymer blends with tunable thermal transitions and mechanical characteristics, Ind. Eng. Chem. Res. 56 (47) (2017) 14069–14077.
[25] L. Cano, D.H. Builes, A. Tercjak, Morphological and mechanical study of nanostructured epoxy systems modified with amphiphilic poly (ethylene oxide-b-propylene oxide-b-ethylene oxide) triblock copolymer, Polymer 55 (3) (2014) 738–745.
[26] W.-C. Chu, W.-S. Lin, S.-W. Kuo, Flexible epoxy resin formed upon blending with a triblock copolymer through reaction-induced microphase separation, Materials 9 (6) (2016) 449.
[27] M. Larrañaga, N. Gabilondo, G. Kortaberria, E. Serrano, P. Remiro, C.C. Riccardi, I. Mondragon, Micro-or nanoseparated phases in thermoset blends of an epoxy resin and PEO–PPO–PEO triblock copolymer, Polymer 46 (18) (2005) 7082–7093.
[28] B. Tang, M. Kong, Q. Yang, Y. Huang, G. Li, Toward simultaneous toughening and reinforcing of trifunctional epoxies by low loading flexible reactive triblock copolymers, RSC Adv. 8 (31) (2018) 17380–17388.
[29] J. Parameswaranpillai, S.K. Sidhardhan, P. Harikrishnan, J. Pionteck, S. Siengchin, A.B. Unni, A. Magueresse, Y. Grohens, N. Hameed, S. Jose, Morphology, thermo-mechanical properties and surface hydrophobicity of nanostructured epoxy thermosets modified with PEO-PPO-PEO triblock copolymer, Polym. Test. 59 (2017) 168–176.
[30] J.S. Jayan, A. Saritha, K. Joseph, Innovative materials of this era for toughening the epoxy matrix: a review, Polym. Compos. 39 (S4) (2018) E1959–E1986.
[31] J. Zhang, D. Zhang, A. Zhang, Z. Jia, D. Jia, Dendritic polyamidoamine-grafted halloysite nanotubes for fabricating toughened epoxy composites, Iran. Polym. J. 22 (7) (2013) 501–510.
[32] J. Luo, S. Yang, L. Lei, J. Zhao, Z. Tong, Toughening, synergistic fire retardation and water resistance of polydimethylsiloxane grafted graphene oxide to epoxy nanocomposites with trace phosphorus, Compos. Part A Appl. Sci. Manuf. 100 (2017) 275–284.
[33] R. Konnola, C.P. Nair, K. Joseph, High strength toughened epoxy nanocomposite based on poly (ether sulfone)-grafted multi-walled carbon nanotube, Polym. Adv. Technol. 27 (1) (2016) 82–89.
[34] J.-Y. Wang, S.-Y. Yang, Y.-L. Huang, H.-W. Tien, W.-K. Chin, C.-C.M. Ma, Preparation and properties of graphene oxide/polyimide composite films with low dielectric constant and ultrahigh strength via in situ polymerization, J. Mater. Chem. 21 (35) (2011) 13569–13575.
[35] H. Roghani-Mamaqani, V. Haddadi-Asl, K. Khezri, M. Salami-Kalajahi, M. Najafi, M. Sobani, S.-A. Mirshafiei-Langari, Confinement effect of graphene nanoplatelets on atom transfer radical polymerization of styrene: grafting through hydroxyl groups, Iran. Polym. J. 24 (1) (2015) 51–62.
[36] R.K. Layek, A.K. Nandi, A review on synthesis and properties of polymer functionalized graphene, Polymer 54 (19) (2013) 5087–5103.
[37] S. Hansson, V. Trouillet, T. Tischer, A.S. Goldmann, A. Carlmark, C. Barner-Kowollik, E. Malmström, Grafting efficiency of synthetic polymers onto biomaterials: a comparative study of grafting-from versus grafting-to, Biomacromolecules 14 (1) (2012) 64–74.
[38] J. Gao, J. Li, S. Zhao, B.C. Benicewicz, H. Hillborg, L.S. Schadler, Effect of graft density and molecular weight on mechanical properties of rubbery block copolymer grafted SiO2 nanoparticle toughened epoxy, Polymer 54 (15) (2013) 3961–3973.
[39] J. Gao, J. Li, B.C. Benicewicz, S. Zhao, H. Hillborg, L.S. Schadler, The mechanical properties of epoxy composites filled with rubbery copolymer grafted SiO2, Polymers 4 (1) (2012) 187–210.

[40] T. Li, S. He, A. Stein, L.F. Francis, F.S. Bates, Synergistic toughening of epoxy modified by graphene and block copolymer micelles, Macromolecules 49 (24) (2016) 9507–9520.
[41] L. Shahriary, A.A. Athawale, Graphene oxide synthesized by using modified hummers approach, Int. J. Renew. Energy Environ. Eng 2 (2014) 58–63, 01.
[42] L. Plangsangmas, J.J. Mecholsky Jr., A.B. Brennan, Determination of fracture toughness of epoxy using fractography, J. Appl. Polym. Sci. 72 (2) (1999) 257–268.
[43] R. Konnola, J. Parameswaranpillai, K. Joseph, Mechanical, thermal, and viscoelastic response of novel in situ CTBN/POSS/epoxy hybrid composite system, Polym. Compos. 37 (7) (2016) 2109–2120.
[44] A. Viinikanoja, J. Kauppila, P. Damlin, M. Suominen, C. Kvarnström, In situ FTIR and Raman spectroelectrochemical characterization of graphene oxide upon electrochemical reduction in organic solvents, Phys. Chem. Chem. Phys. 17 (18) (2015) 12115–12123.
[45] G. Li, P. Li, H. Qiu, D. Li, M. Su, K. Xu, Synthesis, characterizations and biocompatibility of alternating block polyurethanes based on P3/4HB and PPG-PEG-PPG, J. Biomed. Mater. Res. 98 (1) (2011) 88–99.
[46] J.M. Englert, C. Dotzer, G. Yang, M. Schmid, C. Papp, J.M. Gottfried, H.-P. Steinrück, E. Spiecker, F. Hauke, A. Hirsch, Covalent bulk functionalization of graphene, Nat. Chem. 3 (4) (2011) 279.
[47] J.-B. Wu, M.-L. Lin, X. Cong, H.-N. Liu, P.-H. Tan, Raman spectroscopy of graphene-based materials and its applications in related devices, Chem. Soc. Rev. 47 (5) (2018) 1822–1873.
[48] A. Kaniyoor, S. Ramaprabhu, A Raman spectroscopic investigation of graphite oxide derived graphene, AIP Adv. 2 (3) (2012) 32183.
[49] L. Stobinski, B. Lesiak, A. Malolepszy, M. Mazurkiewicz, B. Mierzwa, J. Zemek, P. Jiricek, I. Bieloshapka, Graphene oxide and reduced graphene oxide studied by the XRD, TEM and electron spectroscopy methods, J. Electron. Spectrosc. Relat. Phenom. 195 (2014) 145–154.
[50] J. Liu, Z.J. Thompson, H.-J. Sue, F.S. Bates, M.A. Hillmyer, M. Dettloff, G. Jacob, N. Verghese, H. Pham, Toughening of epoxies with block copolymer micelles of wormlike morphology, Macromolecules 43 (17) (2010) 7238–7243.
[51] B. Qi, S.R. Lu, X.E. Xiao, L.L. Pan, F.Z. Tan, J.H. Yu, Enhanced thermal and mechanical properties of epoxy composites by mixing thermotropic liquid crystalline epoxy grafted graphene oxide, Express Polym. Lett. 8 (7) (2014).
[52] Y. Zhou, L. Li, Y. Chen, H. Zou, M. Liang, Enhanced mechanical properties of epoxy nanocomposites based on graphite oxide with amine-rich surface, RSC Adv. 5 (119) (2015) 98472–98481.
[53] Silva, B.L., Bello, R.H., and Coelho, L.A.F. Role OF triblock copolymers IN The Properties of Epoxy Matrices with Carbon Nanoparticles.
[54] A. Bajpai, B. Wetzel, Effect of different types of block copolymers on morphology, mechanical properties, and fracture mechanisms of bisphenol-F based epoxy system, J. Compos. Sci. 3 (3) (2019) 68.
[55] C.-H. Lee, J.-J. Park, The properties of DSC and DMA for epoxy nano-and-micro mixture composites, Trans. Electr. Electron. Mater. 11 (2) (2010) 69–72.
[56] J.P.B. de Souza, J.M.L. dos Reis, A thermomechanical and adhesion analysis of epoxy/Al2O3 nanocomposites, Nanomater. Nanotechnol. 5 (2015) 18.
[57] I.M. Barszczewska-Rybarek, A. Korytkowska-Wałach, M. Kurcok, G. Chladek, J. Kasperski, DMA analysis of the structure of crosslinked poly (methyl methacrylate) s, Acta Bioeng. Biomech. 19 (1) (2017).
[58] K.W. Putz, M.J. Palmeri, R.B. Cohn, R. Andrews, L.C. Brinson, Effect of cross-link density on interphase creation in polymer nanocomposites, Macromolecules 41 (18) (2008) 6752–6756.
[59] J.D. Liu, H.-J. Sue, Z.J. Thompson, F.S. Bates, M. Dettloff, G. Jacob, N. Verghese, H. Pham, Effect of crosslink density on fracture behavior of model epoxies containing block copolymer nanoparticles, Polymer 50 (19) (2009) 4683–4689.
[60] N.T. Kamar, L.T. Drzal, Micron and nanostructured rubber toughened epoxy: a direct comparison of mechanical, thermomechanical and fracture properties, Polymer 92 (2016) 114–124.
[61] A. Bajpai, B. Wetzel, K. Friedrich, High strength epoxy system modified with soft block copolymer and stiff core-shell rubber nanoparticles: morphology, mechanical properties, and fracture mechanisms, Express Polym. Lett. 14 (4) (2020).
[62] J.S. Oh, J. Suh, J.K. Kim, Floor noise isolation system of the residential buildings using waste rubbers, Appl. Chem. Eng. 28 (4) (2017) 427–431.
[63] Z. Heng, X. Zhang, Y. Chen, H. Zou, M. Liang, In-situ construction of "octopus"-like nanostructure to achieve high performance epoxy thermosets, Chem. Eng. J. 360 (2019) 542–552.
[64] M. Sahu, A.M. Raichur, Toughening of high performance tetrafunctional epoxy with poly (allyl amine) grafted graphene oxide, Compos. B Eng. 168 (2018) 15–24, https://doi.org/10.1016/j.compositesb.2018.12.030.
[65] R. Konnola, J. Joji, J. Parameswaranpillai, K. Joseph, Structure and thermo-mechanical properties of CTBN-grafted-GO modified epoxy/DDS composites, RSC Adv. 5 (76) (2015) 61775–61786.
[66] Y.-J. Wan, L.-C. Tang, L.-X. Gong, D. Yan, Y.-B. Li, L.-B. Wu, J.-X. Jiang, G.-Q. Lai, Grafting of epoxy chains onto graphene oxide for epoxy composites with improved mechanical and thermal properties, Carbon 69 (2014) 467–480.
[67] P. Katti, K.V. Kundan, S. Kumar, S. Bose, Improved mechanical properties through engineering the interface by poly (ether ether ketone) grafted graphene oxide in epoxy based nanocomposites, Polymer 122 (2017) 184–193.
[68] J.S. Jayan, A. Saritha, B.D.S. Deeraj, K. Joseph, Graphene oxide as a prospective graft in Polyethylene glycol for enhancing the toughness of epoxy nanocomposites, Polym. Eng. Sci. (2020).
[69] Y. Liu, S. Chen, S. Ye, J. Feng, A feasible route to balance the mechanical properties of epoxy thermosets by reinforcing a PCL-PPC-PCL toughened system with reduced graphene oxide, Compos. Sci. Technol. 125 (2016) 108–113.
[70] I. Farina, R. Goodall, E. Hernández-Nava, A. di Filippo, F. Colangelo, F. Fraternali, Design, microstructure and mechanical characterization of Ti6Al4V reinforcing elements for cement composites with fractal architecture, Mater. Des. 172 (2019) 107758.
[71] M.M. Khoshhesab, Y. Li, Mechanical behavior of 3D printed biomimetic Koch fractal contact and interlocking, Extrem. Mech. Lett. 24 (2018) 58–65.
[72] Y. Li, C. Ortiz, M.C. Boyce, A generalized mechanical model for suture interfaces of arbitrary geometry, J. Mech. Phys. Solid. 61 (4) (2013) 1144–1167.
[73] L. Djumas, A. Molotnikov, G.P. Simon, Y. Estrin, Enhanced mechanical performance of bio-inspired hybrid structures utilising topological interlocking geometry, Sci. Rep. 6 (2016) 26706.
[74] T. Li, M.J. Heinzer, L.F. Francis, F.S. Bates, Engineering superior toughness in commercially viable block copolymer modified epoxy resin, J. Polym. Sci., Part B: Polym. Phys. 54 (2) (2016) 189–204.
[75] R.M. Hydro, R.A. Pearson, Epoxies toughened with triblock copolymers, J. Polym. Sci., Part B: Polym. Phys. 45 (12) (2007) 1470–1481.